논문 2005-42TC-9-3

실내 아파트 환경에서의 통계적 UWB 채널 모델

(A Statistical Model for the Ultra-Wide Bandwidth Indoor Apartment Channel)

박 진 환*, 이 상 협*, 방 성 일**

(Jin-Hwan Park, Sang-Hyup Lee, and Sung-Il Bang)

요 약

본 논문에서는 실제 아파트 환경에서 2000번의 주파수 응답에 의한 통계적 UWB 실내 채널 모델을 연구하였다. 측정은 서로 다른 방, 서로 다른 위치에서 이루어 졌으며, 실험 결과를 통해 채널의 전파특성을 이론적으로 설명하였다. Time-domain상에서 측정할 수 있는 channel impulse response (CIR)와 frequency-domain상에서 측정할 수 있는 channel transfer function (CTF)의 측정방법을 제안하였다. 측정데이터를 통해서 CIR과 CTF를 비교하여 분석하였고, 통계적 경로손실 모델 또한 제안하였다. 신호 대역은 10MHz에서 8.01GHz까지 사용하였다. 측정결과를 통해 time-domain상에서 확인할 수 있는 maximum excess delay, mean excess delay, rms delay spread를 나타내었다. 송신기와 수신기에는 전방향성의 biconical안테나를 사용하였다. 또한 제안된 아파트 환경에서의 채널 모델은 UWB용 안테나 특성이 포함된 결과이다.

Abstract

We establish a statistical model for the ultra-wide bandwidth (UWB) indoor channel based on over 2000 frequency response measurements campaign in a practical apartment. The approach is based on the investigation of the statistical properties of the multipath profiles measured in different place with different rooms. Based on the experimental results, a characterization of the propagation channel from theoretic view point is described. Also we describe a method for measurement of the channel impulse response and channel transfer function. Using the measured data, the authors compares channel impulse responses obtained from time-domain and channel transfer functions obtained from frequency-domain with statistical path loss model. The bandwidth of the signal used in this experiment is from 10MHz to 8.01GHz. The time-domain results such as maximum excess delay, mean excess delay and rms delay spread are presented. As well as, omni-directional biconical antenna were used for transmitter and receiver. In addition, measurements presented here support UWB channel model including the antenna characteristics.

Keywords: Propagation channel, UWB, Path loss, Mean excess delay, RMS delay spread.

I. Introduction

The physical cornerstone for understanding UWB pulse propagation was established by Sommerfeld a century ago when he attacked the diffraction of a time-domain pulse by a perfectly conducting wedge [1]. Much of the increased attention on UWB technology is due to the landmark ruling by the Federal Communications Commission (FCC) permitted the use of UWB signals within a huge block of spectrum from 3.1GHz to 10.6GHz, i.e. a bandwidth of 7.5GHz, having a 10dB bandwidth larger than 25% of its center frequency, or has 10dB bandwidth equal to or larger than 1.5GHz if the center frequency is greater than 6GHz. Figure 1 shows emission mask of the UWB device[2].

Power spectral density is the main limiting factor

학생회원, ** 정회원, 단국대학교 전자공학과
(Dept. of Electronics & Eng. Dankook University)
※ 본 연구는 중기거점/차세대신기술개발사업 지원으로 수행되었음.
접수일자: 2005년6월17일, 수정완료일: 2005년9월6일

of UWB systems. Therefore, IEEE 802.15.3a targeted application with short range, i.e. under 10m, high data rate, i.e. up to 100Mbps. However, due to implementation limitation, IEEE 802.15.4a, working with the IEEE 802.15.4 MAC layer, received great attention because of reasonable range, i.e. from 100m to 300m, with low data rate, i.e. between 1Kbps and several Mbps.

Amount of appreciable propagation measurements effort have been made over the past few years in different environments, i.e. residential, office, industrial, human body, and agricultural, with both indoor and outdoor channels. Some of the excellent measurement procedures and data reduction techniques with practical environments were work by Win[3], Rappaport[4], Ghassemzadeh[5], Turin[6], Cox[7], and Nielson[8]. However, with few exceptions, including result of professor Win, most of the measurements have been performed for narrow bands which means these measurements are inappropriate for UWB systems.

In our study, from 10MHz to 8.01GHz UWB frequency sweeping method was carried out with VNA and data from DSO are collected in a 200GHz sampling per second.

This paper is organized as follows. Section II introduced the channel measurement technique and the equipment setup presented in this study with experiment procedure. The data post-processing procedure is explained in Section III, along with the best fit procedures that are used to compare the CIR with CTF and to extract the model parameters to develop the statistical model. Finally, conclusions and future works are given in Section IV.

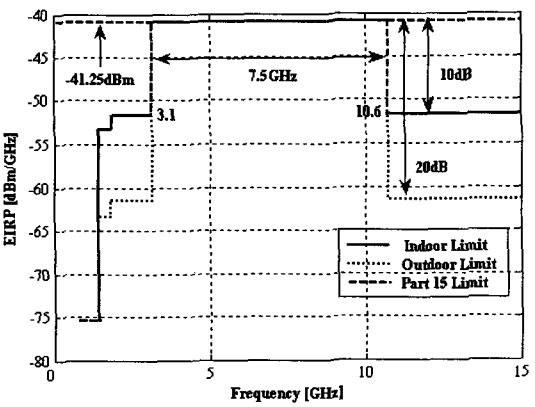

그림 1. 실내 및 핸드헬드용 기기에 대한 UWB 송출 범위

Fig. 1. UWB emission range for indoor and hand-held devices.

II. The UWB Propagation Experiment and Measurement Environment

Generally, there are two possible techniques to perform channel measurements. Firstly, channel can be measured in time-domain in which measurement

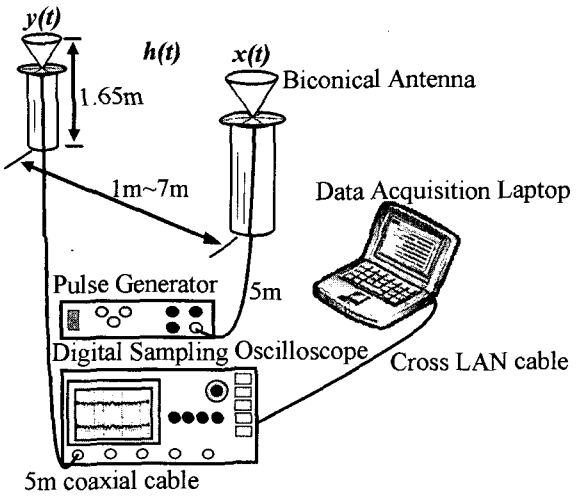

그림 2. 시간영역에서 측정을 위한 블럭 다이어그램

Fig. 2. A block diagram of the time-domain measurement apparatus.

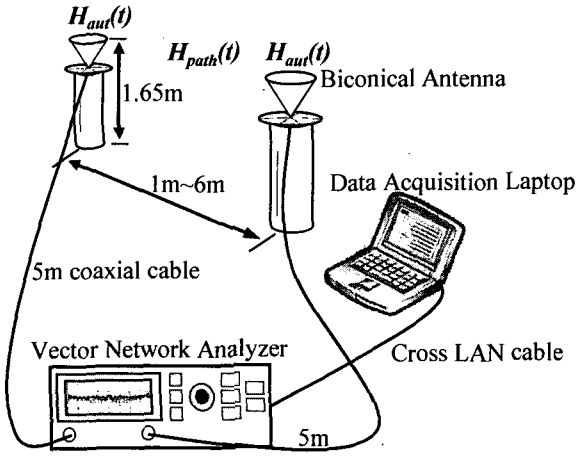

그림 3. 주파수영역에서 측정을 위한 블럭 다이어그램

Fig. 3. A block diagram of the frequency-domain measurement apparatus.

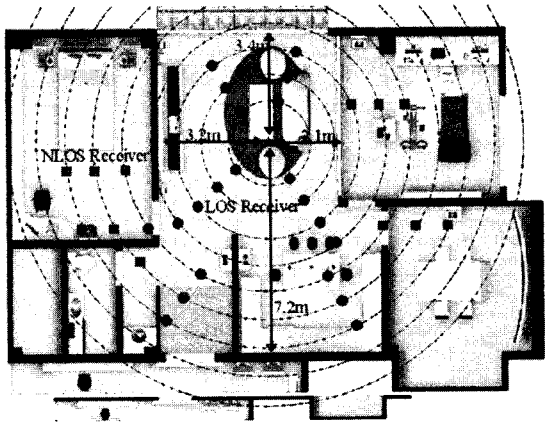

그림 4. 전파측정이 진행된 실제아파트 평면도
Fig. 4. Floor plan of a practical apartment.

usually performed using digital sampling oscilloscope (DSO). This technique measured the channel impulse response (CIR), $h(t)$. The other method is a frequency-domain technique in which measurement usually performed using vector network analyzer (VNA). This technique measured the channel transfer function (CTF), $H(f)$.

In our study, both the frequency-domain and the time-domain measurement system were selected. The ideas for the measurement concepts are presented in Figure 2 and Figure 3. As it will be stated at the end of this paper, theoretically, having a static measurement environment, and a wide bandwidth, both techniques, using DSO and VNA, show up in the same result using FFT or IFFT.

A UWB propagation experiment was performed in a practical apartment having the floor plan shown in Figure 4. The concentric circles are centered on the transmit antenna and are spaced at 1m intervals. Also the photograph of a practical apartment shown in Figure 5.

Time-domain setup consists of a pulse generator that sends pulses to a biconical transmitting antenna through 5m low-loss coaxial cable. The received signal is observed using a DSO (Lecroy wavemaster 8000). The receiver is also a biconical antenna connected to a 5m low-loss coaxial cable. At the same time, DSO is connected to a laptop using LAN cable to acquire data. By experiment, LAN cable is

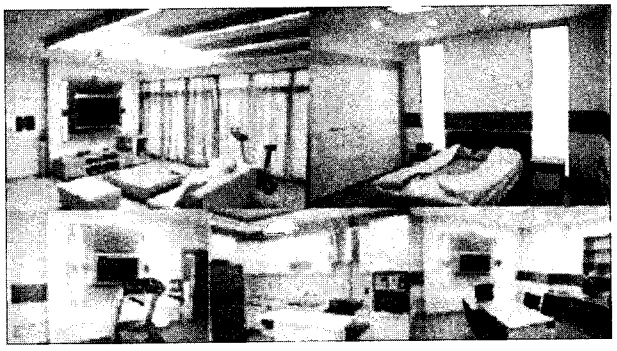

그림 5. 전파측정이 진행된 실제아파트 사진
Fig. 5. Photograph of a practical apartment where the propagation measurement was performed.

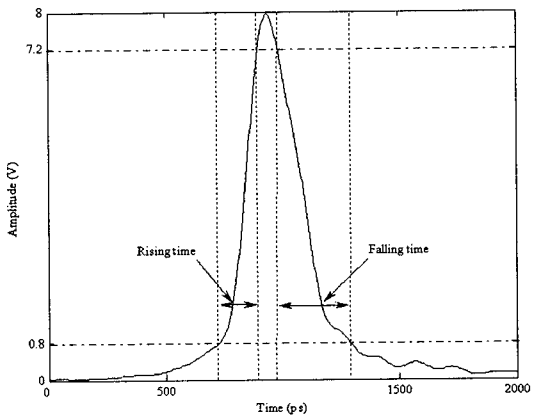

그림 6. 펄스발생기의 펄스 모양
Fig. 6. Pulse shape of pulse generator.

much faster in gathering data than GPIB cable.

From many measurements results, the capacity of UWB system is highly influenced by the selected pulse shape, moreover, by the shape of the pulse width[9]. Transmitted pulse, in this paper, has a slow falling edge which reduces the ringing effects and allows for easier time gating. Transmitted pulse is presented in Figure 6.

Frequency-domain setup is consists of a VNA (Agilent E8363B), pair of biconical antenna connected with 5m same low-loss coaxial cable, and a laptop connect with LAN cable to acquire data. The network analyzer is operated in response measurement mode, where PORT1 and PORT2 is either transmitter or receiver. However, very firstly, the vector network analyzer requires a calibration with the two 5m low-loss coaxial cables and adapters as will be used. This is because of a

표 1. VNA 파라미터값
Table 1. VNA measurements setup parameters.

Parameter		Value
Frequency bandwidth	B	8GHz
Center frequency	f_c	4.01GHz
Delay resolution	$\Delta\tau$	125ps
No. frequency points	N	6401
Frequency step	Δf	1.25MHz
Max. excess delay	$\tau_{\max}$	100.1ns
Sweeping time	t_{sw}	2s
Max. Doppler shift	$f_{d,max}$	0.678Hz

magnitude and phase information of the transmitted signal. Also, important features of the Biconical antenna are omni-directional radiation pattern and a constant phase centre with very wide input impedance bandwidth. Therefore, biconical antennas are a better representative for use in UWB system[13].

Depending on the number of the measured frequency points and on the bandwidth within the sweeping band, the sweeping time is adjusted by authors to 2second with 6401 sampling points. Table 1 lists the main parameters for the frequency-domain using network analyzer. Frequency bandwidth of VNA is 8GHz, i.e. 10MHz to 8.01GHz.

Delay resolution can be defined by frequency bandwidth and is defined as

$$\Delta\tau = 1/B. \tag{1}$$

Maximum limit for the detectable delay of the channel in time domain can be defined by the number of frequency points per a sweep and by the used bandwidth B. Defined by Eq. (2), if the cable lengths exceed the width of the maximum delay window, the calibration algorithm may fail. From Eq. (2),

$$\tau_{\max} = \Delta f/B, \tag{2}$$

numerator part indicates frequency step which can be rewritten as follows:

$$\Delta f = B/(N-1). \tag{3}$$

From Table 1, 100ns corresponds to approximately 30m, which is quite reasonable distance for the indoor environment, especially in apartment. Additionally, to cover correspond space more widely with same frequency bandwidth, authors suggest increasing number of frequency points.

The main reason why many researchers use VNA for the radio channel measurements is the propagation delay in long cables. Long propagation delay will cause the receiver to sample at a frequency that is a little bit higher than the received frequency at the antenna. Technical support from Agilent, frequency shift f_{shift} is a function of the propagation time t_{pt}, the frequency span B, and the sweep time t_{sw}. We write

$$f_{shift} = t_{propagation}\frac{B}{t_{sweep}}, \tag{4}$$

where f_{shift} has to be smaller than IF bandwidth of the analyzer. From Table 1, Eq. (4) yields maximum propagation time approximately 92.4ns.

III. Data Processing and Analysis Results

For measurements conducted using VNA, the CTFs are transformed in the CIRs through inverse Fourier transform (IFFT). Frequency domain windowing is applied prior to the transformation to reduce the leakage problem. Then, the CIRs are analyzed by divided the temporal axis into delay bins or small intervals. This delay bin is corresponding to the width of a path and is determined by the reciprocal of the bandwidth swept, which is time resolution of the measurement system. The CIRs are then normalized such that the total power in each power delay profile (PDP) is equal to one.

In order to compare different multipath channels and to develop some general design guidelines for wireless systems, parameters which grossly quantify the multipath channel are used[11]. The mean excess delay, rms delay spread, and excess delay spread (X dB) are multipath channel parameters that can be determined from a power delay profile. The time

dispersive properties of wide band multipath channels are most commonly quantified by their mean excess delay ($\bar{\tau}$) and rms delay spread (σ_τ). It is important to note that the rms delay spread and mean excess delay are defined from a single power delay profile which is the temporal or spatial average of consecutive impulse response measurements collected and averaged over a local area.

1. Power Delay Profile (PDP)

The *power delay profile* of the channel is found by taking the spatial average of $P(t)=|h(t)|^2$ over a local area.

The measurement results show that the PDP decrease exponentially with excess delay. The time decay constant (TDC) seems to follow a lognormal distribution with 35ns to 40ns for LOS and 43ns to 65ns for NLOS.

2. Mean Excess Delay

The *mean excess delay* is the first moment of the power delay profile and is defined as

$$\bar{\tau} = \frac{\sum_k a_k^2 \tau_k}{\sum_k a_k^2} = \frac{\sum_k P(\tau_k)\tau_k}{\sum_k P(\tau_k)} \tag{5}$$

where a_k, τ_k and $P(\tau_k)$ are the gain coefficient, delay and PDP of the k^{th} multipath component, respectively.

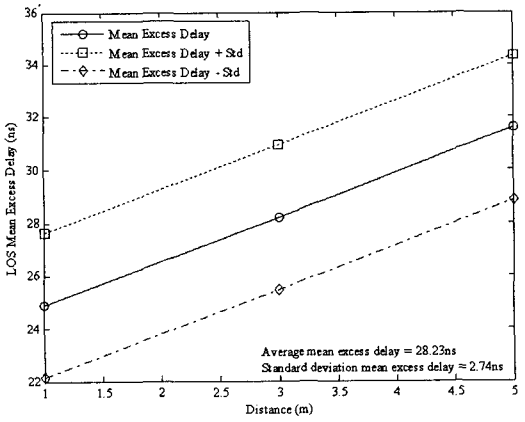

그림 7. LOS환경에서의 mean excess delay
Fig. 7. Mean excess delay of LOS in apartment.

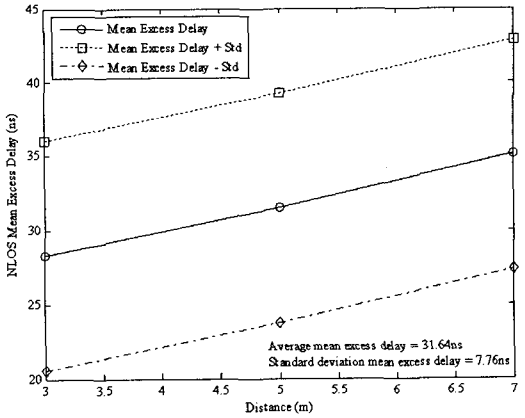

그림 8. NLOS환경에서의 mean excess delay
Fig. 8. Mean excess delay of NLOS in apartment.

The received signal is synchronized at the instant of maximum peak arrival time for detection. If the difference between maximum peak arrival time and mean excess delay is increased then the probability of synchronization error is also increased.

Figure 7 and Figure 8 shows the mean excess delay of LOS and NLOS in apartment with include and exclude the standard deviation. Average mean excess delay and standard deviation mean excess delay also shown in Figures.

3. RMS Delay Spread

The *rms delay spread* is the square root of the second central moment of the power delay profile and is defined by

$$\sigma_\tau = \sqrt{\overline{\tau^2} - (\bar{\tau})^2} \tag{6}$$

where

$$\overline{\tau^2} = \frac{\sum_k a_k^2 \tau_k^2}{\sum_k a_k^2} = \frac{\sum_k P(\tau_k)\tau_k^2}{\sum_k P(\tau_k)} \tag{7}$$

These delays are measured relative to the first detectable signal arriving at the receiver at $\tau_0 = 0$. Therefore the rms delay spread gives information about the dispersiveness of the wireless channel and it highly influence the channel transmission error[12].

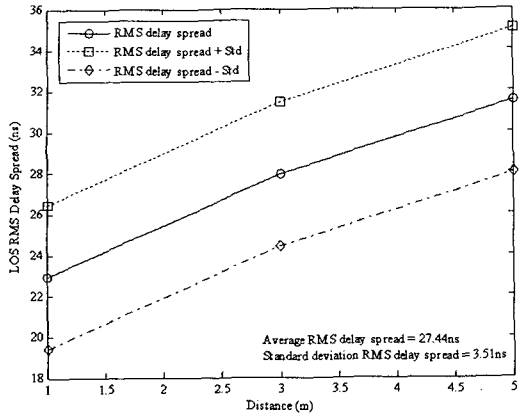

그림 9. LOS환경에서의 RMS delay spread
Fig. 9. RMS delay spread of LOS with average and standard deviation.

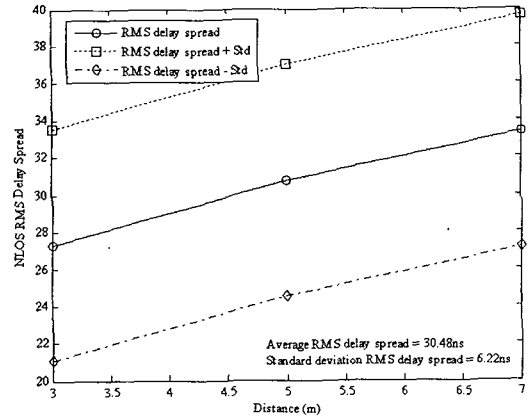

그림 10. NLOS환경에서의 RMS delay spread
Fig. 10. RMS delay spread of NLOS with average and standard deviation.

Figure 9 and Figure 10 shows the rms delay spread of LOS and NLOS in apartment with include and exclude the standard deviation. Average mean excess delay and standard deviation mean excess delay also shown in Figures.

4. Maximum Excess Delay

The *maximum excess delay* (X dB) of the power delay profile is defined to be the time delay during which multipath energy falls to X dB below the maximum. In other words, the maximum excess delay is defined as $\tau_X - \tau_0$, where τ_0 is the first arriving signal and τ_X is the maximum delay at which a multipath component is within X dB of the strongest arriving multipath signal. Therefore, the received power which is smaller than this level is considered as noise in the communication system. The maximum excess delay also gives characteristics of the channel which relate to the communication error.

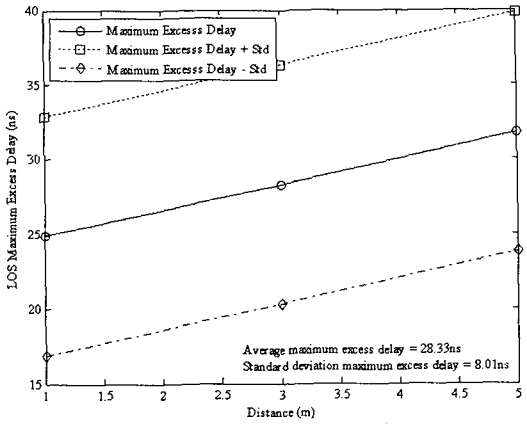

그림 11. LOS환경에서의 maximum excess delay
Fig. 11. Maximum excess delay of LOS in apartment.

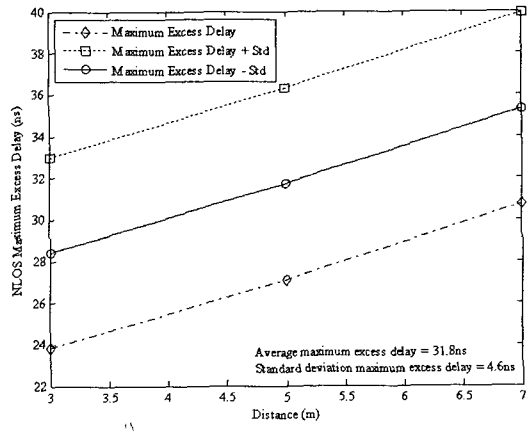

그림 12. NLOS환경에서의 maximum excess delay
Fig. 12. Maximum excess delay of NLOS in apartment.

표 2. 10dB 임계치 내에서의 power, mean excess delay, 그리고 RMS delay spread
Table 2. Percent of power contained in profile, mean excess delay ($\overline{\tau}$), RMS delay spread (σ_τ) for 10dB threshold.

LOS			NLOS		
power	$\overline{\tau}$(ns)	σ_τ(ns)	power	$\overline{\tau}$(ns)	σ_τ(ns)
89.2%	28.23	27.44	86.4%	31.64	30.48

Figure 11 and Figure 12 shows the maximum excess delay of LOS and NLOS in apartment with include and exclude the standard deviation. Average maximum excess delay and standard deviation maximum excess delay also shown in Figures.

A summary of these values is given in Table 2. The results showed that the mean excess delay and rms delay spread increases as expected.

5. Path Loss

The path loss usually denotes the local average received signal power relative to the transmit power. In realistic radio channels, free space does not apply. A general path loss model uses a parameter, n, to denote the power law relationship between distance and received power. From Eq. (8),

$$\overline{PL}(d) \propto (\frac{d}{d_0})^n, \tag{8}$$

where $\overline{PL}$ is the mean path loss, n is the path loss exponent which indicates how fast path loss increases with distance(n=2 for free space propaga tion). d_0 is a reference distance, and d is the transmitter and receiver separation distance[14].

The distance dependence of the path loss in decibels is described by

$$\overline{PL}(d)[dB] = PL_0[dB] + 10 \times n \times \log(\frac{d}{d_0}) \tag{9}$$

where the reference distance d_0 is set to 1m, and PL_0 is the path loss at reference distance. n is the path loss exponent.

The path loss exponent also depends on the environment where experiment were peformed, and on whether a line-of-sight (LOS) connection exists between the transmitter and receiver or not. LOS path loss exponents in indoor environments range from 1m in a corridor to about 2 in an office environment. NLOS exponents typically range from 3 to 4 for soft NLOS, and 4 to 7 for hard NLOS[10].

From Eq. (9), typical values of path loss exponents and standard deviations for LOS and NLOS are given in Table 3.

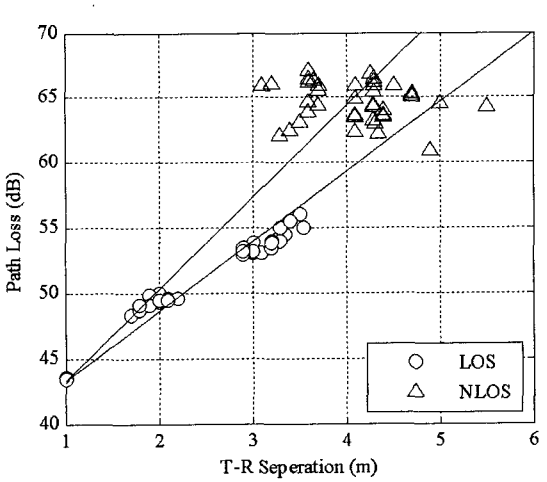

그림 13. 송신기와 수신기 사이에서의 경로손실
Fig. 13. Scatter plot of path loss versus transmitter and receiver separation.

표 3. 경로손실 지수와 표준편차 값
Table 3. Path loss exponent and standard deviation measured in apartment.

Parameter	LOS		NLOS	
	Mean	S.D	Mean	S.D
PL_0[dB]	43.5	NA	64.2	NA
n	2.1	0.1	3.5	0.7

Figure 13 shows the scatter plot of the path loss as a function of transmitter and receiver separation for apartment. This straight line provides the mean value of the random path loss.

6. Group delay

The phase linearity of the communication channel can be specified in terms of group delay[15]. The group delay is the rate of change of phase shift with respect to angular frequency, as the wave progress through the wireless channel. Traditionally, group delay has been used to describe the propagation delay and examine deviation from conventional linear phase characteristics of systems. This parameter also contains valuable information about wireless wave propagation delay and distortion through nonlinear communication channel.

Mathematically, group delay, t_g, is the derivative of the phase response and is represented by

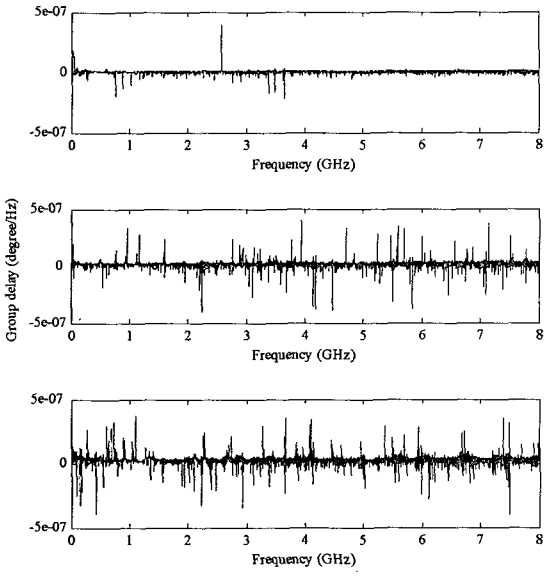

그림 14. LOS 1m, 3m, 5m 에서의 group delay
Fig. 14. Group delay of LOS 1m, 3m, 5m in degrees/Hz.

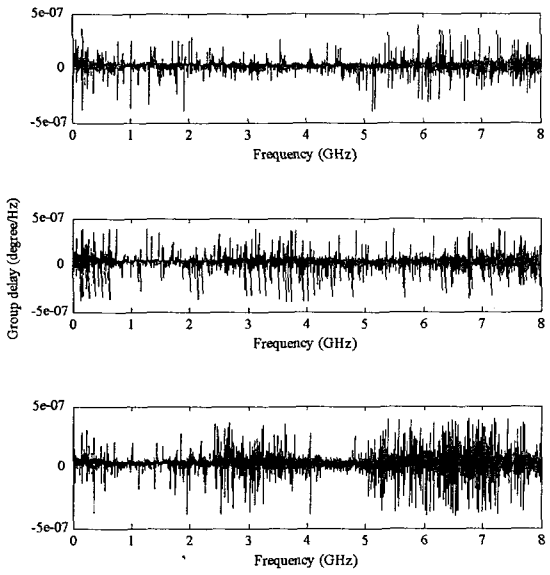

그림 15. NLOS 3m, 5m, 7m 에서의 group delay
Fig. 15. Group delay of NLOS 3m, 5m, 7m in degrees/Hz.

$$t_g = -\frac{\Delta\phi}{360\Delta f} \tag{10}$$

where $\Delta\phi$ is the phase difference in degrees at two frequencies separated by Δf in Hz. The Δf is commonly called the aperture of the measurement.

The group delay may be considered as the time delay of the amplitude envelope of a sine wave at frequency ω.

The VNA calculated group delay from its phase response measurement. Figure 14 shows the group delay with LOS 1m, 3m, 5m and also Figure 15 shows the group delay with NLOS 3m, 5m, 7m.

There are three pass bands clearly seen in the group delay response of LOS 1m, one is between 0.4GHz to 0.75GHz and secondly in the 1.6GHz to 2.65GHz and lastly between 3.7GHz to 8.01GHz. In these pass bands, the phase is observed to be linearly dependent on frequency. According to Figure 14 and Figure 15, as TR-separation get longer, pass band from group delay get shorter. Also NLOS group delay has less pass band than LOS group delay.

Ⅳ. Conclusions

In this paper, the channel transfer function (CTF) is measured using the frequency seep method using a vector network analyzer and the channel impulse response (CIR) is calculated by filtering the transfer function and taking an inverse Fourier transform (IFFT).

The channel impulse response is the multipath signal with delayed and attenuated. The delayed and attenuated pattern depends on both the communication system and the wireless channel itself. The power delay profile (PDP) has been used to describe the delay and attenuation pattern in a apartment channel. PDP delay parameters such as mean excess delay, RMS delay spread, maximum excess delay are calculated using the measured CIRs in the practical apartment.

Finally, the effect of furniture such as desks and chairs in each room, the impact of floors, ceiling, windows, walls are identified in the CIR. The CIR is parametrically characterized using the conventional delay parameters such as the mean excess delay and the RMS delay spread value.

V. Acknowledgement

The authors wish to thank Dr. Yong-Jin Park, researcher in the Korea Electrotechnology Research Institute (KERI), who encouraged, guided and pointed in the right direction with educating. Also like to appreciate Jong-Hwa Song and Myung-O Kim for unsparing assistance and support for the propagation measurement experiments.

Reference

[1] Terence W. Barrertt, "History of UltraWideBand (UWB) Radar & Commun.: Pioneers and Innovat ors," Proc. in Electromagnetics Symposium 2000.

[2] FCC Document 00-163: Revision of Part 15 of the Commission's Rules Regarding Ultra-Wide band Transmission Systems, April 22, 2002, ET Docket No. 98-153.

[3] M.Z.Win and R.A.Scholtz, "Characterization of ultra-wide bandwidth wireless indoor channels: a communication-theoretic view," *IEEE J. Select. Areas Commun.*, vol. 20, no. 9, pp. 1613-1627, Dec. 2002.

[4] Theodore S. Rappaport, "Characterization of UHF multipath radio channels in factory buildings," *IEEE Trans. Antennas Propagat.*, vol. AP-37, no. 8, pp. 1058-1069, Aug. 1989.

[5] S.S.Ghassemzadeh, R.Jana, C.Rice, W.Turin, and V.Tarokh, "Measurement and modeling of an ultra-wide bandwidth indoor channel," *IEEE Trans. Commun.*, in press.

[6] G.L.Turin, "Introduction to spread-spectrum anti multipath techniques and their application to urban digital radio," *in Proc. IEEE*, vol. 68, no. 3, pp. 328-353, Mar. 1980.

[7] Donald C.Cox, "910MHz urban mobile radio propagation: Multipath characteristics in New York City," *IEEE Trans. Commun.*, vol. COM 21, no. 11, pp. 1188-1194, Nov. 1973.

[8] Donald L.Nielson, "Microwave propagation measurements for mobile digital radio application," *IEEE Trans. on Vehicul. Technol.*, vol. VT-28, no. 3, pp. 117-132, Aug. 1978.

[9] Jin Hwan Park, Bag Geun Bae, Young Eun Ko, and Sung I Bang, "Structure proposal of the TDMG pulse generator for single band UWB systems," in *Proc. IEEE Industrial Electronics Society 30th Annual Conf.* Nov. 2004, Busan, Korea, 2004.

[10] J.Keignart and N.Daniele, "Channel sounding and modeling for indoor UWB communications," *International Workshop on Ultra Wide Band Systems 2003.*

[11] T.S. Rappaport, *Wireless Communications: Principles and Practices,* Prentice Hall, 2002.

[12] JTE McDonnell, TP Spiller, and TA Wilkinson, "RMS delay spread in indoor LOS environments at 5.2 GHz," *IEE. Electronics Letters,* vol. 34, no. 11, pp. 1149-1150, May 1998.

[13] Z. Irahhauten, H. Nikookar, G.J.M. Janssen, "An Overview of Ultra Wide Band Indoor Channel Measurements and Modeling", *IEEE Microwave and Wireless Components Letters,* Vol. 14, No. 8, pp. 386-388, August 2004.

[14] A.H. Muqaibel, A. Safaai-Jazi, A.M. Attiya, A. Bayram, and S.M. Riad, "Measurements and Characterization of Indoor UWB Propagation" *2nd IEEE Conference on Ultra Wideband Systems and Technologies,* p.p. 295-299, Nov. 2003.

[15] Agilent Technologies, "User Guide, Agilent Technologies 8753ES Option 011 Network Analyzer", Part Number: 08753-90479, June 2002.

저 자 소 개

박 진 환(정회원)
2004년 건국대학교
전자공학과 학사 졸업
2004년 3월~현재 단국대학교
전자공학과 석사 과정
<주관심분야 : UWB, RF Amp, 디지털통신>

방 성 일(정회원)
1984년 단국대학교 공과대학
전자공학전공 (공학사)
1986년 단국대학교 대학원
전자공학전공 (공학석사)
1992년 단국대학교 대학원
전자공학전공 (공학박사)
1992년~1993년 (주)대기정보통신 책임연구원
1997년~현재 단국대학교
전기전자컴퓨터공학부 교수
2001년~현재 단국대학교 산학연 센터장
2003년~현재 ICSUN 기술고문
<주관심분야 : RF Amp, UWB, 디지털통신>

이 상 협(정회원)
2004년 3월~현재 단국대학교
전자공학과 석사 과정
<주관심분야 : UWB, FDTD, RF Amp>